

A Unified Framework for Input Feature Attribution Analysis

Jingyi Sun Pepa Atanasova Isabelle Augenstein

University of Copenhagen

{jisu, pepa, augenstein}@di.ku.dk

Abstract

Explaining the decision-making process of machine learning models is crucial for ensuring their reliability and fairness. One popular explanation form highlights key input features, such as i) tokens (e.g., Shapley Values and Integrated Gradients), ii) interactions between tokens (e.g., Bivariate Shapley and Attention-based methods), or iii) interactions between spans of the input (e.g., Louvain Span Interactions). However, these explanation types have only been studied in isolation, making it difficult to judge their respective applicability. To bridge this gap, we propose *a unified framework that facilitates a direct comparison between highlight and interactive explanations* comprised of four diagnostic properties¹. Through extensive analysis across these three types of input feature explanations—each utilizing three different explanation techniques—across two datasets and two models, we reveal that each explanation type excels in terms of different diagnostic properties. In our experiments, highlight explanations are the most faithful to a model’s prediction, and interactive explanations provide better utility for learning to simulate a model’s predictions. These insights further highlight the need for future research to develop combined methods that enhance all diagnostic properties.

1 Introduction

Input feature explanations reveal how a model makes decisions based on the input for which the prediction is made. Among these, *Token Explanations* (TokenEx; e.g., Shapley Values (Lundberg and Lee, 2017) and Integrated Gradients (Sundararajan et al., 2017)) are widely used to assign importance scores to specific segments of the input, such as tokens in natural language processing tasks. However, complex reasoning tasks usually require reasoning across multiple pieces of text,

¹We make the code for the framework available at <https://github.com/copenlu/A-unified-framework-for-highlight-explanations>.

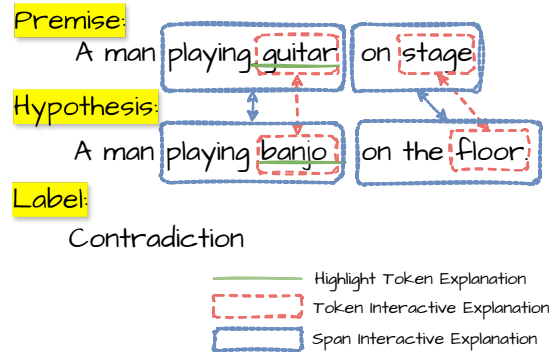


Figure 1: An example of the three types of Input Feature Explanations on an instance from the SNLI dataset, with their two most important pieces of explanation (token, token tuple, span tuple, correspondingly).

e.g., Fact Checking is performed given a claim and evidence, Natural Language Inference is performed given a premise and a hypothesis, where Token Explanations can be insufficient to present the relations employed between the different parts of the input. To this end, *Token Interactive Explanations* (TokenIntEx; e.g., Bivariate Shapley (Masoomi et al., 2023), and Layer-wise Attention Attribution (Ye et al., 2021)) provide importance scores for interactions between two tokens of the input. Further, to enhance the semantic coherence of these explanations, *Span Interactive Explanations* (SpanIntEx; e.g., Louvain community detection (Ray Choudhury et al., 2023) model interactions across tuples of input spans. An example showcasing these three types of input feature explanations is given in Figure 1.

It is crucial to develop rigorous and comprehensive evaluation frameworks to ensure the principled selection of the most suitable explanation in a practical application (Yu et al., 2024) and systematic progress in the development of different types of explanations (Atanasova et al., 2022; Jolly et al., 2022). However, these input feature explanations

have typically been studied in isolation, with few exceptions, where explanation methods of the same type are compared (Atanasova et al., 2020; DeYoung et al., 2020; Janizek et al., 2021; Ray Choudhury et al., 2023). Moreover, evaluations of interactive explanations have been restricted to one property. To address these gaps, we propose *a unified framework that facilitates a direct comparison between highlight and interactive input feature explanations on a suite of four diagnostic properties.*

Unified Evaluation Framework. Our unified evaluation framework consists of four essential diagnostic properties – Faithfulness, Agreement with Human Annotation, Simulatability, and Complexity. They are the most widely used for Token explanations and include the only property used for interactive explanations – Faithfulness. *Faithfulness* (Chen et al., 2020, 2021; Ray Choudhury et al., 2023) measures the extent to which explanations accurately reflect the actual reasons used by the model in its predictions. *Agreement with Human Annotation* (Atanasova et al., 2020) evaluates whether explanations exhibit an inductive bias akin to human reasoning, potentially enhancing their plausibility to end users. *Simulatability* (Pruthi et al., 2022) estimates whether the explanations are useful to an agent for replicating the model’s decisions. Finally, *Complexity* (Bhatt et al., 2021) evaluates whether the explanations are easy to comprehend by presenting distinctive key features rather than a uniform distribution of importance scores. Crucially, we propose *extensions of these properties* such that they can be applied to different types of input feature explanations – token (TokenEx), two tokens (TokenIntEx), or more than two tokens (SpanIntEx).

Characterising Input Feature Explanations. We conduct an extensive analysis across two different tasks and language models, and three different explanation techniques for each input feature explanation type. Our findings indicate that TokenEx explanations exhibit greater faithfulness than SpanIntEx and TokenIntEx explanations. Additionally, SpanIntEx and TokenIntEx explanations align more closely with human annotations at the token level compared to TokenEx explanations. Moreover, SpanIntEx explanations demonstrate higher interaction overlap with human annotations than TokenIntEx explanations. Further, SpanIntEx explanations are found to be most beneficial for agent simulatability. Fi-

nally, our results suggest that SpanIntEx and TokenEx explanations tend to be easier to comprehend.

Overall, our extensive analysis reveals the varied strengths of each explanation type across different diagnostic properties. These insights underscore the importance of developing integrated methods that combine the different types of explanations to enhance all diagnostic properties in future research.

2 A Unified Evaluation Framework for Highlight Explanations

To systematically compare feature attribution explanations of different types, we present a unified framework comprised of four widely employed diagnostic properties: Faithfulness, Agreement with Human Annotations, Simulatability, and Complexity. This section formally introduces these properties and outlines our proposed extensions to allow for their application across different input feature explanation types.

2.1 Preliminaries

We start with a dataset D , and a model M fine-tuned on D . An instance $x \in D$ is comprised of two parts, e.g., a claim and an evidence, the first consisting of m tokens, and the second – of n tokens. We apply an explanation attribution method A_E of type $E \in \{\text{TokenEx}, \text{TokenIntEx}, \text{SpanIntEx}\}$ to M , and each instance $x \in D$: $A_E(M, x) = \{e_k^x, a_k^x | k \in [0, s - 1]\}$, where e_k^x is a span/a pair of spans from the input and a_k^x denotes its importance score. k is the importance ranking of the corresponding piece of explanation. s is an upper limit for the number of most important pieces of explanation for an instance, such that: $s \in [1, m + n]$ for TokenEx, $s \in [1, m \cdot n]$ for TokenIntEx, and for SpanIntEx s varies for each instance with $s \in [1, f]$, $f < m! \cdot n!$. Depending on the explanation type E , e_k^x can consist of: one token x_i for TokenEx, $i \in [0, m + n - 1]$, one token pair (x_p, x_q) for TokenIntEx, where $p \in [0, m - 1]$ and $q \in [m, m + n - 1]$, one span pair $((x_s, \dots, x_{s+l_1}), (x_t, \dots, x_{t+l_2}))$ for SpanIntEx, where $s, s + l_1 \in [0, m - 1]$ and $t, t + l_2 \in [m, m + n - 1]$.

Considering a particular threshold for the number of most important explanation pieces s , we compute the total set of input tokens involved in

the presented explanation for x :

$$T_{E,M}(x, s) = \{x_i | x_i \in e_k^x, k \in [0, s - 1]\} \quad (1)$$

When computing the different diagnostic properties, previous works have adopted a range of thresholds s . Moreover, as noted above, the maximum possible value for s can vary across different types of input feature explanations. Additionally, the number of tokens included in the top- k important explanations can differ substantially among explanation types: in top-1 we can have: in a top-1 setting, the explanations consist of 1 token for `TokenIntEx`, 2 tokens for `TokenIntEx`, and more than 2 tokens for `SpanIntEx` (Ray Choudhury et al., 2023; DeYoung et al., 2020). This variability makes it difficult to compare results across different explanation types. To address this problem, we propose extensions for each of the studied diagnostic properties that result in **unified diagnostic properties** which can be used for a direct comparison of the different types of input feature explanations.

2.2 Faithfulness

Faithfulness (DeYoung et al., 2020) assesses whether explanations accurately reflect the model’s decision-making process. It involves two aspects – Comprehensiveness and Sufficiency – measured as the number of the model’s prediction changes after keeping (SP) or omitting (CP) k of the most important portions of the input, respectively:

$$CP(x, E, k) = \left\{ \begin{array}{ll} 0, & \text{if } f(x - T_{E,M}(x, k)) = f(x) \\ 1, & \text{otherwise} \end{array} \right\} \quad (2)$$

$$SP(X, E, k) = \left\{ \begin{array}{ll} 1, & \text{if } f(T_{E,M}(x, k)) = f(x) \\ 0, & \text{otherwise} \end{array} \right\} \quad (3)$$

To take different thresholds k , we average over $k \in [0, s = m + n - 1]$. We then also average the results across instances within D to compute the final Comprehensiveness/Sufficiency score:

$$Comp_E/Suff_E = \frac{\sum_{x \in D} \sum_{k=0}^s CP/SP(x, E, k)}{|D|} \quad (4)$$

Unified Faithfulness. To facilitate the comparison of faithfulness scores, we introduce a **dynamic threshold** $\theta_{x,k}$. This threshold represents the number of unique tokens used for a perturbation on input x , same across all explanation types. Since top- k explanations from `SpanIntEx` typically contain more tokens than `TokenEx` or `TokenIntEx`, the number of tokens in top- k `SpanIntEx` explanations sets the number of unique tokens used for

perturbations across all types of input feature explanations:

$$\theta_{x,k} = |T_{SpanIntEx,M}(x, k)| \quad (5)$$

Thus, $\theta_{x,k}$ becomes a dynamic threshold that adapts based on each instance’s top- k `SpanIntEx` explanation tokens. We then adjust the number of top- k explanations selected from `TokenEx` and `TokenIntEx`, $k_{TokenEx}$ and $k_{TokenIntEx}$, correspondingly, to result in the same number of perturbed tokens $\theta_{x,k}$:

$$|T_{TokenEx,M}(x, k_{TokenEx}(x))| = \theta_{x,k} \quad (6)$$

$$|T_{TokenIntEx,M}(x, k_{TokenIntEx}(x))| = \theta_{x,k} \quad (7)$$

Furthermore, a *Random baseline* is established, where the tokens for perturbation are selected randomly so that it matches the average $\theta_{x,k}$ across D .

2.3 Agreement with Human Annotation

Agreement with Human Annotation has been used to assess the overlap between generated and human-annotated `TokenEx` explanations (Atanasova et al., 2020), which can indicate the plausibility of the generated explanations to end users. For $E = \text{TokenEx}$, the measure is computed by calculating a precision score for the top- k most important explanations compared to the gold Human Annotations.

For $E = \text{TokenEx}$, s are explanations extracted from instance x , where $s = m + n$, s thresholds are set corresponding to each explanation’s attribution score, forming the threshold list $\omega_E(x)$:

$$\omega_E(x) = [a_0^x, \dots, a_s^x] \quad (8)$$

By selecting explanations with higher attribution scores than each threshold in $\omega_E(x)$, s targeted explanation sets are obtained, where $C_E(x, i)$ represents the set for the i^{th} threshold:

$$C_E(x, i) = \{e_j^x : a_j^x \leq a_i^x\} \quad (9)$$

Comparing these sets with the golden explanation set e^G , s precision-recall pairs can be derived. Average Precision (AP) is then obtained by weighting the precision value with the corresponding recall increase:

$$P_i/R_i(x, e^G, E) = Pre/Rec(C_E(x, i), e^G) \quad (10)$$

$$AP_E(x, e^G) = \sum_{i=0}^s (R_i - R_{i-1}) * P_i \quad (11)$$

Finally, Mean AP (MAP) is calculated by averaging AP across the instances in the dataset D :

$$MAP_E = \frac{\sum_{x \in D} AP_E(x, e^G)}{|D|} \quad (12)$$

Unified Agreement with Human Annotation Measure. For a fair comparison between the different types of explanations, the thresholds $\omega_E(x)$ for including the same number of tokens across the different types of explanations follows the procedure set in the Unified Faithfulness property (§2.2). In particular, we start with the thresholds set for SpanIntEx, and adjust the thresholds for TokenEx/TokenIntEx to reach the same number corresponding number of tokens. Furthermore, we measure agreement with human annotations at the **interaction level** for the gold SpanIntEx/TokenIntEx explanations and at the **token level** for gold TokenEx explanations.

Interaction-level Agreement with Human Annotation. For a fair comparison between TokenIntEx and SpanIntEx explanations, we adapt MAP_{TokenEx} to the interaction level.

We compute the mean average precision (Eq. 12) w.r.t. the human-annotated TokenIntEx/SpanIntEx sets.

Token-level Agreement with Human Annotation. For a fair comparison between TokenEx and TokenIntEx/SpanIntEx explanations, we extract tokens from TokenIntEx/SpanIntEx explanations and compare them with tokens from golden TokenIntEx/SpanIntEx explanations. The threshold lists $\omega_{\text{TokenIntEx/SpanIntEx}}(x)$ are used, but the targeted sets $C_{E_{\text{token}}}(x, i)$ contain tokens extracted from TokenIntEx/SpanIntEx, correspondingly.

The golden set $S_{E_{\text{token}}}(x)$ aggregates tokens from golden TokenIntEx/SpanIntEx explanations. The token-level agreement scores $MAP_{\text{TokenIntEx}_{\text{token}}}/MAP_{\text{SpanIntEx}_{\text{token}}}$ accordingly, following the procedure set for MAP_{TokenEx} (Eq. 12).

We also set a *Random baseline*, where the number of randomly selected span pairs, token pairs, or tokens for each instance matches the average number of SpanIntEx explanations per instance across all attribution methods.

2.4 Simulatability

Simulatability was initially proposed to measure how accurately humans can predict a model’s out-

puts based on its explanations (Chen et al., 2023). Previous studies have demonstrated that Simulatability can be approximated using an automated agent model as a surrogate for human understanding (Pruthi et al., 2022). *Given the established positive correlation between Simulatability and human evaluation of explanation utility from previous research*, we integrate the Simulatability scores obtained from the agent model with different explanation types to approximate their utility for humans.

In prior research, an agent model AM , sharing the same architecture as the original model M , was introduced. AM was trained to simulate M ’s predictions Y' using post-hoc TokenEx explanations. During AM ’s training phase, the top- k explanations extracted for M were provided as additional signals. In comparison, another agent model, AM_O , was trained without explanation guidance as a baseline on the same training set. During the testing phase, the simulation accuracy of both AM and AM_O over the shared dataset D is calculated. The difference between their accuracies is interpreted as the explanation’s effect in enhancing the original model’s simulatability:

$$Sim = ACC(AM(D), Y') - ACC(AM_O(D), Y') \quad (13)$$

Unified Simulatability. To compare the simulation utility of different explanation types, we train a separate agent model, denoted as AM_E , for each explanation type E , and calculate the corresponding simulation performance on the common test set. For a fair comparison across the different explanation types, we first ensure top- k_E explanations are presented for assisting the agent’s training for explanations type E , following the same method stated in Section §2.2. This approach ensures that each model is exposed to the same quantity of explanation information, specifically the number of unique tokens from the different explanation types.

During the training phase of the agent model, we introduce the explanations of type E respectively into the learning of AM_E ; we supplement the input sequence x with top- k_E explanations instead so that the agent model will be trained with the same mechanism whether the explanations are provided or not, and each training instance will contain the input sequence x_E and golden label Y' which is predicted by the original model M . Specifically, we examine two different ways of presenting the explanations as part of the original input sequence, named I_{Symbol} and I_{Text} ; all aim to ensure the ex-

planations of different types are inserted similarly. See the details of insertion forms in Appendix A.

At test time, the F1 scores of all agent models – AM_E and AM_O , over the shared dataset D are calculated. Note that the explanations of type E are also provided to the input for the unseen instances for agent model AM_E . The difference between each agent model AM_E and AM_O on simulation performance is the final metric indicating how much this specific type of input feature explanation enhances the model’s simulatability, noted as RSF_E .

$$SF_E = F1(AM_E(x_E), Y'), x \in D \quad (14)$$

$$SF_O = F1(AM_O(x), Y'), x \in D \quad (15)$$

$$RSF_E = SF_E - SF_O \quad (16)$$

2.5 Complexity

Feature attribution explanations are designed to aid human understanding of a model’s reasoning over specific instances. However, since humans have a limited capacity to process large amounts of information simultaneously, these explanations need to be easy to comprehend. Even if we select only the top- k attributions with the highest importance scores, they need to be distinctive as opposed to the attribution scores having a uniform distribution.

To measure this complexity of attribution scores, [Bhatt et al. \(2021\)](#) employ entropy ([Rényi, 1961](#)) over the attribution scores of all the produced highlight explanations. Higher entropy means different features have similar attribution scores, where the simplest explanation, with low entropy, would be concentrated on one feature. The calculation process is noted as follows, where $m+n$ is the total number of generated `TokenEx` explanations, and all explanations are considered for the complexity score computation.

$$P(x, p) = \frac{|a_p^x|}{\sum_{q=1}^{m+n} |a_q^x|} \quad (17)$$

$$CL(X) = - \sum_{p=1}^{m+n} P(x, p) \ln(P(x, p)) \quad (18)$$

Unified Complexity. Building on their approach, we also employ Entropy to measure the complexity of explanation attribution scores across different types of input feature explanations. To ensure a fair comparison, we maintain consistency in the size of the chosen explanation lists across all types for the

same instance, denoted as k_x , as the number of generated `TokenEx/TokenIntEx/SpanIntEx` explanations vary for the same instance. The complexity score of the top- k_x explanation list under type E , denoted as $CL_E(x, k_x)$, is calculated as:

$$P_E(x, k_x, i) = \frac{|a_i^x|}{\sum_{j=1}^{k_x} |a_j^x|} \quad (19)$$

$$CL_E(x, k_x) = - \sum_{i=1}^{k_x} P_E(x, k_x, i) \ln(P_E(x, k_x, i)) \quad (20)$$

where a_i^x/a_j^x represent the i/j th highest attribution score from the explanation set for x . $P_E(x, k_x, i)$ is the fraction of the attribution score of the i th most important explanation compared to the sum of the scores within all the top k_x chosen explanations.

Finally, by applying this calculation of the complexity score regarding explanation attribution lists for type E to all instances, we obtain the complexity score of each explanation type as CL_E .

$$CL_E = \frac{\sum_{x \in D} CL_E(x, k_x)}{|D|} \quad (21)$$

Notably, we calculate k_x using the number of `SpanIntEx` explanations within the instance, as the number of explanations of this type is unknown until they are generated, as discussed in §2.1.

3 Experimental Setup

3.1 Datasets

We select the natural language inference dataset SNLI ([Bowman et al., 2015](#)), where instances consist of a premise, a hypothesis, and a label $y \in \{entailment, neutral, contradiction\}$. Additionally, we select the fact checking dataset FEVER ([Thorne et al., 2018](#)), where instances consist of a claim, an evidence, and a label $y \in \{entailment, neutral, contradiction\}$. For generating the input feature explanations, we sample 4000 instances from each train, dev, and test set due to the computational requirements especially pronounced for Shapley-based explanations ([Atanasova et al., 2020](#)). To evaluate agreement with human annotations, we describe in Appendix B the datasets used, which contain various types of input feature explanations for SNLI and FEVER annotated by humans.

3.2 Input Feature Explanation Methods

To generate importance scores, as techniques for `TokenEx` we select three common explanation

techniques – Shapley (Lundberg and Lee, 2017), Attention (DeYoung et al., 2020), and Integrated Gradients (IG, Sundararajan et al. (2017)). For `TokenIntEx`, we employ Bivariate Shapley (Masoomi et al., 2023), Attention (Clark et al., 2019), and Layer-wise Attention Attribution (Ye et al., 2021). Following Ray Choudhury et al. (2023), we apply the Louvain algorithm (Blondel et al., 2008) on top of each of the three selected `TokenIntEx` to generate importance scores for `SpanIntEx`, where the importance score of each span interaction is averaged over the importance scores of the token interactions within it.

Notably, the techniques applied for generating `TokenIntEx` are the bivariate version of the techniques used for generating `TokenEx`; e.g. Layer-wise Attention Attribution uses IG. Furthermore, `SpanIntEx` are generated from importance scores of `TokenIntEx`. We will refer to Shapley, Attention, and IG as the explanation base types used for generating all types of input feature explanations for brevity. See the details of generating all input feature explanations with different explainability techniques in Appendix D.

3.3 Models

We use the BERT-base-uncased model (Devlin et al., 2019) with 12 encoder layers, and the BART-base-uncased model (Lewis et al., 2020) with 6 encoder and 6 decoder layers, as common representatives of the encoder and the encoder-decoder Transformer architecture (Vaswani et al., 2017). Our model choice is particularly influenced by the substantial computational requirements of the input feature explanations, especially pronounced for Shapley (Atanasova et al., 2020). Additionally, our choice is guided by the need to directly access the models’ internals for generating IG and Attention-based explanations. Furthermore, while our framework currently utilizes the said models, it is designed to be easily adaptable to other models or newly developed explainability techniques, provided that there are more robust computational resources available.

We fine-tune the base models on SNLI and FEVER and use them to generate explanations. Their performance on the corresponding test sets is shown in Appendix C. For the Simulation property, we follow existing work (Fernandes et al., 2022; Pruthi et al., 2022) and train simulator agent models (see §2.4) with the same architectures as the

base ones. Following Fernandes et al. (2022), we split the test set into train/dev/test for the training of the agent model that simulates the original model’s predictions.

4 Results and Discussion

We now present the results of our unified evaluation framework (§2) illustrated in Figure 2. Our results include span the input feature explanations `SpanIntEx`, `TokenIntEx`, and `TokenEx` (§3.2), two models (§3.3), two datasets (§3.1), and three base explanation techniques per input feature explanation type (§3.2). For Simulatability, we select the results of I_{sym} , as this form avoids repeating the input text and increasing the input size substantially. For Agreement with Human Annotation, we select the results of Token-level agreement as they are present for all types of explanations. Appendix E lists all detailed results per property.

4.1 Faithfulness

Unified Comprehensiveness. Across both datasets and models, *TokenEx* and *TokenIntEx* are identified as the most comprehensive explanation types, achieving the highest scores in 7/12 and 5/12 cases, respectively. `SpanIntEx`, designed to enhance the semantic coherence of interactive explanations by including additional context, often incorporates tokens that do not directly contribute to the model’s prediction, thus explaining its lower comprehensiveness scores. Compared to the random baseline, `TokenEx` and `SpanIntEx` always outperform it, while `TokenIntEx` mostly underperforms it when based on IG. Across the base explanation techniques, `TokenEx` performs best when based on Attention for BERT and on Shapley for BART, indicating that *different base explanation techniques can perform better for different architectures*. Both `TokenIntEx` and `SpanIntEx` show optimal performance when based on Shapley and Attention. Overall, the results indicate a *stronger performance of Attention and Shapley over IG* across all explanation types.

Unified Sufficiency. *SpanIntEx* ranks as the most sufficient explanation type in 7/12 cases, surpassing `TokenEx`, which performs well in only 3/12 cases. While contrary to `SpanIntEx` Comprehensiveness performance, we attribute this to the semantic coherence of the extracted top spans, which provide more meaningful information. Un-

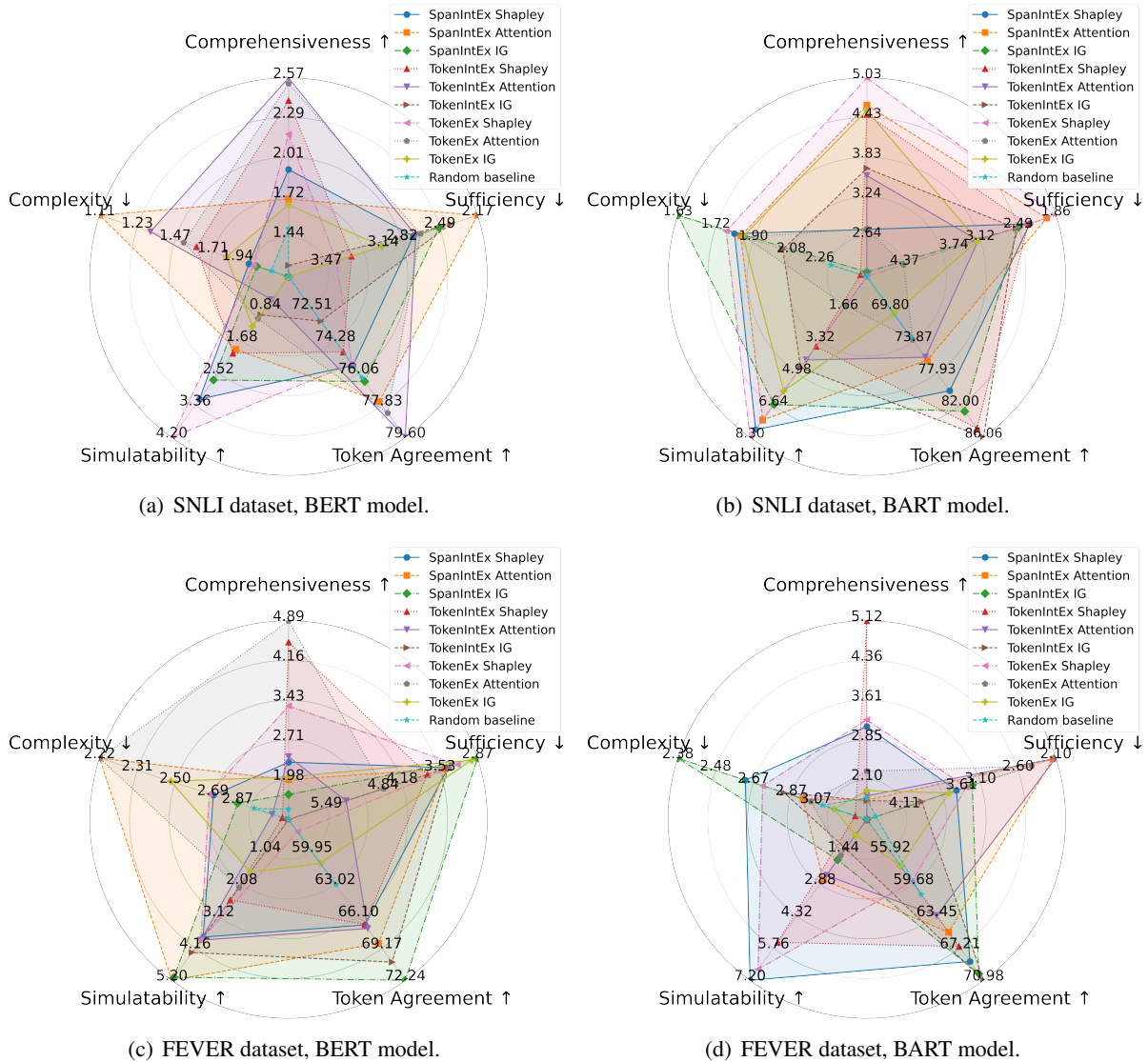


Figure 2: Unified evaluation framework (§2) results for all feature attribution methods (§3.2).

like TokenEx, which consistently outperforms the random baseline, TokenIntEx and SpanIntEx struggle to outperform it on FEVER, likely due to the longer input length compared to SNLI, posing more challenges for the explanations to accurately unveil the model’s internal processes. The results from different base explanation techniques show no clear trends, indicating a *significant variability stemming from the specific dataset and model architecture*.

4.2 Agreement with Human Annotation

In comparing token-level agreement, SpanIntEx and TokenIntEx show higher agreement scores with human annotations than TokenEx. Similarly, we find that SpanIntEx consistently achieves higher agreement with human interaction-level an-

notators, especially when based on Attention scores (see Appendix E). This indicates that *SpanIntEx is more plausible to humans than the other types of explanations due to their enhanced semantics coherence*. In contrast, TokenEx often scores lower than the random baseline. Moreover, considering SpanIntEx’s lower performance in terms of Comprehensiveness, there emerges a *distinct trade-off between comprehensiveness and plausibility*. Across the base explanation techniques, IG performs best for the FEVER dataset; IG and Attention perform best for SNLI. In addition, we find that for the interaction-level agreement, TokenIntEx and SpanIntEx perform worst when based on Shapley. The lower agreement results for Shapley compared to its better comparative performance on Comprehensiveness, once again indicate an exist-

ing trade-off between the two properties.

4.3 Simulatability

Our results show that `SpanIntEx` achieves the highest simulatability in 9/12 cases, helping the agent model accurately reproduce the original model’s predictions. This again underscores the critical role of contextual information and enhanced semantic coherence provided by `SpanIntEx` explanations. Notably, providing `SpanIntEx` explanations to agents improves their ability to simulate the original model by up to 7.9 F1 points compared to scenarios without explanations. Among the base explanation techniques, IG consistently performs best for `SpanIntEx`; other techniques do not exhibit a clear trend.

4.4 Complexity

`SpanIntEx` and `TokenEx` generally achieve similar complexity scores, which consistently remain lower than those of `TokenIntEx`. This suggests that `TokenEx` and `SpanIntEx` generate more distinctive attribution scores, potentially making them easier for humans to understand. Regarding the base explanation techniques, Attention consistently yields the best complexity scores for BERT across all explanation types. There is however no clear trend for BART. Additionally, as detailed in Appendix E, `TokenIntEx` frequently underperforms compared to a random baseline, highlighting its complexity.

4.5 Overall

In sum, we find that while `TokenEx` and `TokenIntEx` generally provide more comprehensive insights, `SpanIntEx` performs better in Sufficiency due to its enhanced semantic coherence, and despite occasionally including irrelevant tokens (§4.1). We find that there exists a trade-off between comprehensiveness and the plausibility of explanations (§4.2), suggesting that the most faithful explanations, and in turn, the model’s actual inner workings can be less plausible to end users.

Furthermore, `SpanIntEx` significantly helps for Simulatability, allowing agents to accurately replicate model decisions (§4.3), which is crucial for practical applications. The Complexity analysis (§4.4) shows that `SpanIntEx` and `TokenEx` are easier to comprehend compared to `TokenIntEx`, underscoring the importance of selecting explanation techniques that cater to the specific needs of the dataset and model architecture.

5 Related Work

Input Feature Explanations. Considerable research exists on extracting explanations from input data. Methods like perturbation-based attribution (e.g., Shapley (Lundberg and Lee, 2017)), attention-based methods (e.g., Attention (Jain and Wallace, 2019; Serrano and Smith, 2019)), and gradient-based methods (e.g., Integrated Gradients (Sundararajan et al., 2017; Serrano and Smith, 2019)) are prevalent for highlighting individual tokens. As individual tokens lack interaction information and thus might be insufficient to explain the model, many attribution methods have been extended to bivariate forms (Masoomi et al., 2023; Janizek et al., 2021; Sundararajan et al., 2017; Ye et al., 2021) to capture input token interactions. More recent work has explored how groups of tokens collectively contribute to model reasoning (Ray Choudhury et al., 2023; Chen et al., 2021). Unlike other work where token groups might consist of tokens from arbitrary positions, Ray Choudhury et al. (2023) introduces a method to explicitly capture span interactions, enhancing the comprehensiveness of explanations by containing the entire spans.

Explanation Evaluation. For evaluating `TokenEx` explanations, DeYoung et al. (2020); Atanasova et al. (2020) propose metrics to measure how faithful explanations are to the model’s inner reasoning. They also propose to assess the plausibility of explanations to humans by measuring the agreement of `TokenIntEx` with human annotations. To assess the utility of explanations to humans, Pruthi et al. (2022) propose to use an agent model as a proxy for humans and evaluate whether explanations aid in model simulatability. Complexity Bhatt et al. (2021) measures the distribution of attribution scores of `TokenEx` and assesses whether the key tokens in token explanations are easily comprehensible to humans. To evaluate `TokenIntEx` most works adopt the faithfulness or axiomatic/theoretical path (Tsang et al., 2020; Sundararajan et al., 2020; Janizek et al., 2021). Current work on evaluating `SpanIntEx` explanations has primarily focused on faithfulness (Ray Choudhury et al., 2023). However, since `SpanIntEx`, `TokenIntEx`, and `TokenEx` explanations contain varying amounts of tokens, which e.g. affects the faithfulness test, this makes direct comparisons between different explanation types using existing metrics challenging. To our knowledge, no prior paper has involved all types of input feature expla-

nations within a unified evaluation framework.

6 Conclusion

We introduced a unified evaluation framework for input feature attribution analysis to guide the principled selection of the most suitable explainability technique in practical applications. Our analysis outlines the diverse strengths and trade-offs among `TokenEx`, `TokenIntEx`, and `SpanIntEx`. Our findings particularly underscore `SpanIntEx`'s superior agreement with human inductive biases and its enhancement of Simulatability, despite its lower comprehensiveness in capturing the model's reasoning compared to `TokenEx` and `TokenIntEx`. This study emphasizes the importance of selecting explanation techniques tailored to specific datasets and model architectures. Future efforts should focus on developing combined methods that enhance both the faithfulness and user comprehensibility of explanations.

Limitations

Our work introduces a unified framework to evaluate input feature explanations across four key properties. We generated three types of explanations using three attribution methods on two transformer models (BERT-base and BART-base) for two NLU tasks (NLI and fact-checking). This enabled us to assess and compare the properties of each explanation type. Due to computational resource limitations, we did not include larger decoder-only models in our evaluation. Future research could explore these models to provide additional insights. Additionally, examining the properties of different explanations in various tasks beyond NLI and fact-checking would be valuable.

Our findings indicate that span interactive explanations (`SpanIntEx`) have a notable advantage over other types in Agreement with Human Annotation, Simulatability, and Complexity, suggesting they are easier for humans to understand. This insight could inspire future work to leverage `SpanIntEx` as the input feature explanation in HCI models. However, `SpanIntEx` shows low comprehensiveness in faithfulness evaluations. The Louvain algorithm, used for `SpanIntEx` generation, may limit its comprehensiveness despite using different attribution methods for `TokenIntEx`. Future work should explore better methods for capturing span interactions and possibly combine `SpanIntEx` and `TokenEx` for higher faithful-

ness, as `TokenEx` demonstrates a stable advantage in comprehensiveness.

Another core finding is that the attribution method significantly affects most diagnostic properties of all explanation types, such as sufficiency. No single attribution method consistently excels across all properties, highlighting the need for continuous evaluation and improvement in attribution methods, particularly for `SpanIntEx`.

Acknowledgements

 This research was co-funded by the European Union (ERC, ExplainYourself, 101077481), by the Pioneer Centre for AI, D NRF grant number P1, as well as by The Villum Synergy Programme (grant number 40543). Views and opinions expressed are however those of the author(s) only and do not necessarily reflect those of the European Union or the European Research Council. Neither the European Union nor the granting authority can be held responsible for them.

References

- Pepa Atanasova, Jakob Grue Simonsen, Christina Lioma, and Isabelle Augenstein. 2020. [A Diagnostic Study of Explainability Techniques for Text Classification](#). In *Proceedings of the 2020 Conference on Empirical Methods in Natural Language Processing (EMNLP)*, pages 3256–3274, Online. Association for Computational Linguistics.
- Pepa Atanasova, Jakob Grue Simonsen, Christina Lioma, and Isabelle Augenstein. 2022. [Diagnostics-Guided Explanation Generation](#). *Proceedings of the AAAI Conference on Artificial Intelligence*, 36(10):10445–10453.
- Umang Bhatt, Adrian Weller, and José M. F. Moura. 2021. Evaluating and Aggregating Feature-based Model Explanations. In *Proceedings of the Twenty-Ninth International Joint Conference on Artificial Intelligence, IJCAI'20*.
- Vincent D Blondel, Jean-Loup Guillaume, Renaud Lambiotte, and Etienne Lefebvre. 2008. Fast Unfolding of Communities in Large Networks. *Journal of statistical mechanics: theory and experiment*, 2008(10):P10008.
- Samuel Bowman, Gabor Angeli, Christopher Potts, and Christopher D Manning. 2015. A Large Annotated Corpus for Learning Natural Language Inference. In *Proceedings of the 2015 Conference on Empirical Methods in Natural Language Processing*, pages 632–642.

- Oana-Maria Camburu, Tim Rocktäschel, Thomas Lukasiewicz, and Phil Blunsom. 2018. E-SNLI: Natural Language Inference with Natural Language Explanations. *Advances in Neural Information Processing Systems*, 31.
- Hanjie Chen, Song Feng, Jatin Ganhotra, Hui Wan, Chulaka Gunasekara, Sachindra Joshi, and Yangfeng Ji. 2021. Explaining Neural Network Predictions on Sentence Pairs via Learning Word-Group Masks. In *Proceedings of the 2021 Conference of the North American Chapter of the Association for Computational Linguistics: Human Language Technologies*, pages 3917–3930.
- Hanjie Chen, Guangtao Zheng, and Yangfeng Ji. 2020. Generating Hierarchical Explanations on Text Classification via Feature Interaction Detection. In *Proceedings of the 58th Annual Meeting of the Association for Computational Linguistics*, pages 5578–5593.
- Yanda Chen, Ruiqi Zhong, Narutatsu Ri, Chen Zhao, He He, Jacob Steinhardt, Zhou Yu, and Kathleen McKeown. 2023. Do Models Explain Themselves? Counterfactual Simulatability of Natural Language Explanations. *arXiv e-prints*, pages arXiv–2307.
- Kevin Clark, Urvashi Khandelwal, Omer Levy, and Christopher D. Manning. 2019. [What Does BERT Look at? An Analysis of BERT’s Attention](#). In *Proceedings of the 2019 ACL Workshop BlackboxNLP: Analyzing and Interpreting Neural Networks for NLP*, pages 276–286, Florence, Italy. Association for Computational Linguistics.
- Jacob Devlin, Ming-Wei Chang, Kenton Lee, and Kristina Toutanova. 2019. BERT: Pre-training of Deep Bidirectional Transformers for Language Understanding. In *Proceedings of the 2019 Conference of the North American Chapter of the Association for Computational Linguistics: Human Language Technologies, Volume 1 (Long and Short Papers)*, pages 4171–4186.
- Jay DeYoung, Sarthak Jain, Nazneen Fatema Rajani, Eric Lehman, Caiming Xiong, Richard Socher, and Byron C Wallace. 2020. ERASER: A Benchmark to Evaluate Rationalized NLP Models. In *Proceedings of the 58th Annual Meeting of the Association for Computational Linguistics*, pages 4443–4458.
- Patrick Fernandes, Marcos Treviso, Danish Pruthi, André Martins, and Graham Neubig. 2022. Learning to Scaffold: Optimizing Model Explanations for Teaching. *Advances in Neural Information Processing Systems*, 35:36108–36122.
- Sarthak Jain and Byron C. Wallace. 2019. [Attention Is Not Explanation](#). In *Proceedings of the 2019 Conference of the North American Chapter of the Association for Computational Linguistics: Human Language Technologies, Volume 1 (Long and Short Papers)*, pages 3543–3556, Minneapolis, Minnesota. Association for Computational Linguistics.
- Joseph D Janizek, Pascal Sturmfels, and Su-In Lee. 2021. Explaining Explanations: Axiomatic Feature Interactions for Deep Networks. *Journal of Machine Learning Research*, 22(104):1–54.
- Shailza Jolly, Pepa Atanasova, and Isabelle Augenstein. 2022. Generating Fluent Fact Checking Explanations with Unsupervised Post-editing. *Information*, 13(10):500.
- Mike Lewis, Yinhan Liu, Naman Goyal, Marjan Ghazvininejad, Abdelrahman Mohamed, Omer Levy, Veselin Stoyanov, and Luke Zettlemoyer. 2020. BART: Denoising Sequence-to-Sequence Pre-training for Natural Language Generation, Translation, and Comprehension. In *Proceedings of the 58th Annual Meeting of the Association for Computational Linguistics*, pages 7871–7880.
- Scott M Lundberg and Su-In Lee. 2017. A Unified Approach to Interpreting Model Predictions. *Advances in neural information processing systems*, 30.
- Aria Masoomi, Davin Hill, Zhonghui Xu, Craig P Hersh, Edwin K Silverman, Peter J Castaldi, Stratis Ioannidis, and Jennifer Dy. 2023. Explanations of Black-box Models Based on Directional Feature Interactions. *arXiv preprint arXiv:2304.07670*.
- Danish Pruthi, Rachit Bansal, Bhuwan Dhingra, Livio Baldini Soares, Michael Collins, Zachary C. Lipton, Graham Neubig, and William W. Cohen. 2022. [Evaluating Explanations: How Much Do Explanations from the Teacher Aid Students?](#) *Transactions of the Association for Computational Linguistics*, 10:359–375.
- Sagnik Ray Choudhury, Pepa Atanasova, and Isabelle Augenstein. 2023. [Explaining Interactions Between Text Spans](#). In *Proceedings of the 2023 Conference on Empirical Methods in Natural Language Processing*, pages 12709–12730, Singapore. Association for Computational Linguistics.
- Alfréd Rényi. 1961. On Measures of Entropy and Information. In *Proceedings of the fourth Berkeley symposium on mathematical statistics and probability, volume 1: contributions to the theory of statistics*, volume 4, pages 547–562. University of California Press.
- Sofia Serrano and Noah A Smith. 2019. Is Attention Interpretable? In *Proceedings of the 57th Annual Meeting of the Association for Computational Linguistics*, pages 2931–2951.
- Mukund Sundararajan, Kedar Dhamdhere, and Ashish Agarwal. 2020. The Shapley Taylor Interaction Index. In *International conference on machine learning*, pages 9259–9268. PMLR.
- Mukund Sundararajan, Ankur Taly, and Qiqi Yan. 2017. Axiomatic Attribution for Deep Networks. In *International conference on machine learning*, pages 3319–3328. PMLR.

- James Thorne, Andreas Vlachos, Christos Christodoulopoulos, and Arpit Mittal. 2018. FEVER: A Large-scale Dataset for Fact Extraction and VERification. In *Proceedings of the 2018 Conference of the North American Chapter of the Association for Computational Linguistics: Human Language Technologies, Volume 1 (Long Papers)*, pages 809–819.
- Michael Tsang, Sirisha Rambhatla, and Yan Liu. 2020. How Does This Interaction Affect Me? Interpretable Attribution for Feature Interactions. *Advances in neural information processing systems*, 33:6147–6159.
- Ashish Vaswani, Noam Shazeer, Niki Parmar, Jakob Uszkoreit, Llion Jones, Aidan N Gomez, Łukasz Kaiser, and Illia Polosukhin. 2017. [Attention Is All You Need](#). In *Advances in Neural Information Processing Systems*, volume 30. Curran Associates, Inc.
- Xi Ye, Rohan Nair, and Greg Durrett. 2021. [Connecting Attributions and QA Model Behavior on Realistic Counterfactuals](#). In *Proceedings of the 2021 Conference on Empirical Methods in Natural Language Processing*, pages 5496–5512, Online and Punta Cana, Dominican Republic. Association for Computational Linguistics.
- Haeun Yu, Pepa Atanasova, and Isabelle Augenstein. 2024. Revealing the Parametric Knowledge of Language Models: A Unified Framework for Attribution Methods. In *Proceedings of the 62nd Annual Meeting of the Association for Computational Linguistics*.

A Detailed Explanation Insertion Method

To enable a fair comparison among different input feature explanations in terms of simulatability (§2.4), we applied consistent insertion formats to combine the explanations with the original input for training the agent models. This design aims to minimize noise from insertion format differences. We tested two ways, each applicable to all types of input feature explanations, to construct input sequences with inserted explanations of type E . These input sequences are denoted x_E in §2.4, omitting specific insertion format details for brevity.

For Symbol-Insertion I_{Symbol} , we preserve the original input sequence but insert special symbols $<$ and $>$ to quote the tokens (for `TokenEx` and `TokenIntEx`) or spans (for `SpanIntEx`) within the input. Additionally, for `TokenEx`, we append a ranking mark after each quoted token based on their attribution scores, ranked in descending order. For `TokenEx` and `SpanIntEx`, each quoted token/span is also assigned a ranking mark indicating the rank of their respective interactions by attribution score, ensuring tokens/spans from the same interaction share the same mark. This method allows us to generate input sequences combined with different input feature explanations in a consistent symbol insertion format.

For Text-Insertion I_{Text} , we append tokens, token tuples, or span tuples to the end of the original input sequence for each explanation type. They are added in the order ranked by descending attribution score. Specifically, for `TokenEx`, tokens from different `TokenEx` explanations are separated by semicolons. For `TokenIntEx` and `SpanIntEx`, tokens/spans within each interaction are connected by a comma, and different interactions are separated by semicolons. This approach constructs input sequences combined with each type of input feature explanation in a consistent text insertion format.

B Agreement Dataset Details

To assess how different types of input feature explanations overlap with human annotations, we collected golden explanations of various types from e-SNLI and *SpanEx* for instances within the SNLI and FEVER datasets, respectively. Detailed information about the annotated explanation types and the number of instances with labeled explanations for these datasets is shown in

D	E	Size
SNLI	-	549367 Train
		9842 Dev
		9824 Test
e-SNLI	TokenEx	549367 Train
		9842 Dev
		9824 Test
<i>SpanEx-SNLI</i>	SpanIntEx TokenIntEx	3865 Test
FEVER	-	145449 Train
		9999 Dev
		9999 Test
<i>SpanEx-FEVER</i>	SpanIntEx TokenIntEx	3206 Test

Table 1: Overview of datasets SNLI (Bowman et al., 2015), FEVER (Thorne et al., 2018), *SpanEx* (Ray Choudhury et al., 2023) and e-SNLI (Camburu et al., 2018). *SpanEx* contains instances from SNLI and FEVER datasets, annotated with `SpanIntEx` explanations including token-level explanations (`TokenIntEx` explanations). e-SNLI contains instances from SNLI dataset, annotated with `TokenEx` explanations.

Table 1. For the SNLI dataset, e-SNLI provides `TokenEx` explanations, while *SpanEx-SNLI* includes `SpanIntEx` explanations and token-level interactions (`TokenIntEx` explanations). We selected 3,865 overlapping instances and evaluated the human agreement score for different types of input feature explanations. For the FEVER dataset, *SpanEx-FEVER* includes `SpanIntEx` and token-level interactions (`TokenIntEx` explanations). Since no `TokenEx` explanations are provided, we extracted tokens from the golden `TokenIntEx` explanations in *SpanEx-FEVER* as an approximation. These selected instances are also used when evaluating other properties of input feature explanations.

C Base Model Performance.

As shown in Table 2, we report the performance of fine-tuned BERT-base and BART-base models on the SNLI and FEVER datasets, respectively. These models, fine-tuned for their specific tasks, are used to generate various input feature explanations through different explainability techniques. Importantly, these are the original models that the agent models, as described in §2.4, learn to simulate.

Model	F1 score	
	Dev	Test
BERT-SNLI	87.21	88.43
BART-SNLI	86.81	85.40
BERT-FEVER	86.21	89.49
BART-FEVER	85.19	84.88

Table 2: The performance of our BERT-base and BART-base models fine-tuned on SNLI and FEVER datasets, respectively, regarding F1 score(%).

D Explainability Techniques

In this section, we detail the explainability techniques employed to generate various types of input feature explanations. As outlined in §3.2, we categorize these techniques based on the method used for generating TokenEx, while TokenIntEx explanations stem from their bivariate variants, forming the basis for SpanIntEx explanations.

Shapley. To assign importance scores to each token within the input, we employ the SHAP method following Lundberg and Lee (2017), utilizing Kernel SHAP to approximate Shapley values. For token interactions, we apply Bivariate Shapley (Mansoori et al., 2023) to assess a token’s influence to model prediction in the presence of another token, particularly when they originate from different parts of the input. The importance score for each token interaction is derived by averaging these mutual influence scores between the involved tokens. With these importance scores for all possible token interactions, we apply the Louvain algorithm (Ray Choudhury et al., 2023) to identify clusters of neighboring token interactions characterized by dense intra-cluster and sparse inter-cluster relationships, which collectively form span interactions. The importance score for each span interaction is calculated by averaging the importance scores of the token interactions it comprises.

Attention. For each token within the input sequence, we use the self-attention weights between this token and the first token as an indicator of its importance score (Jain and Wallace, 2019). We follow Ray Choudhury et al. (2023) to select the most important attention head in the last layer of the model to obtain these attention weights. For each possible token interaction, we use the method by Clark et al. (2019) to extract and average the attention weights between token pairs from different parts of the input to derive their importance scores, also from the most important head of the last layer.

E	Shap	Att	IG	Rand
Interaction level agreement				
SpanIntEx	30.18	57.40	39.40	33.82
TokenIntEx	29.02	37.02	35.06	23.42
TokenEx	-	-	-	-
Token level agreement				
SpanIntEx	75.63	78.26	76.52	76.96
TokenIntEx	74.89	79.60	73.19	74.96
TokenEx	75.54	77.62	70.74	76.33

Table 3: Human Annotation Agreement Results (see §2.3) on SNLI dataset when explanations are generated based on BERT. Interaction-level and Token-level agreement scores, Average Precision(%), compared to human annotations for explanation types SpanIntEx, TokenIntEx, TokenEx generated by Shapley(**Shap**), Attention(**Att**), Integradiant Gradients(**IG**) respectively. Using the same attribution method, the highest alignment score for each category is highlighted in bold. **Rand** indicates the random baseline as described in §2.3.

To obtain span interactions and assign them importance scores, we apply the same method to these token interaction scores as described above.

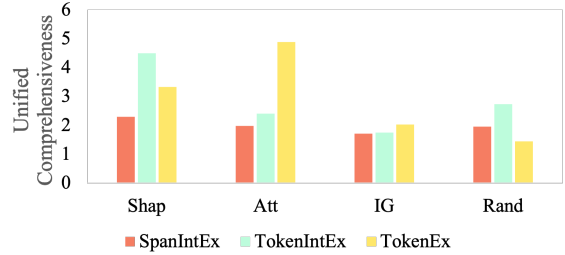
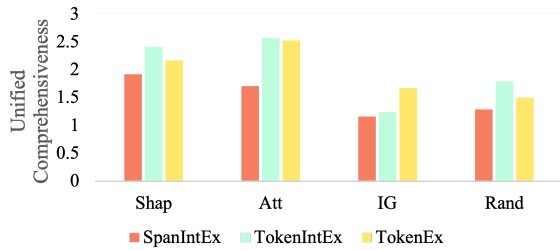
Integrated Gradients. To calculate the importance score for each token in the input sequence, we integrate the gradients of the model’s output with respect to each token embedding, following Sundararajan et al. (2017). For generating the importance scores of token interactions, we use Layer-wise Attention Attribution (Ye et al., 2021), which attributes attention links between pairs of tokens within attention maps with a mechanism similar to Integrated Gradients. These attribution maps are created for each model layer and then aggregated across layers to form a final attribution map. The importance score for each token interaction is calculated as the average value from this final attribution map between the involved tokens. For span interactions, we generate and assign importance scores using the same approach based on the importance scores of the token interactions.

E Detailed Experiment Results

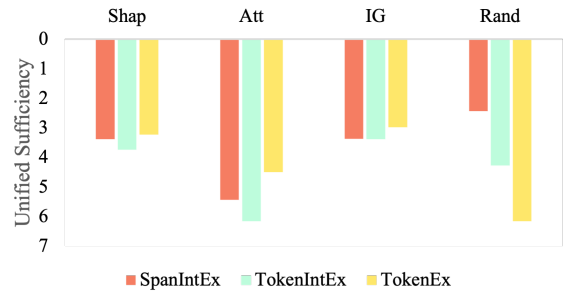
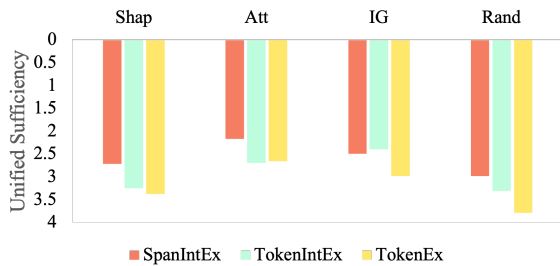
E.1 Faithfulness

E.2 Agreement with Human Annotation

There is a notable gap between interaction-level and token-level agreement scores. For example, in Table 3, the highest interaction-level agreement score for SpanIntEx explanations is 57.40%, while the highest token-level agreement score for SpanIntEx is 78.26%. A similar pattern is ob-



(a) Comprehensiveness on SNLI dataset, the higher the better. (b) Comprehensiveness on FEVER dataset, the higher the better.



(c) Sufficiency on SNLI dataset, the lower the better.

(d) Sufficiency on FEVER dataset, the lower the better.

Figure 3: Unified Comprehensiveness and Sufficiency of three types of feature attribution explanations on SNLI and FEVER datasets using the BERT model. Subfigures (a) and (c) show Unified Comprehensiveness results, while (b) and (d) show Unified Sufficiency results. Explanations are generated by Shapley (Shap), Attention (Att), and Integrated Gradients (IG). Randomly selected span pairs, token pairs, and tokens are baselines corresponding to explanation type SpanIntEx, TokenIntEx, and TokenEx and form the group Random baseline (Rand). We set $k = 3$ for top span interactions and adjust token counts as per §2.2, also ensuring the random baseline matches the average token count of the top k span interactions.

E	Shap	Att	IG	Rand
Interaction level agreement				
SpanIntEx	19.92	28.12	27.45	19.33
TokenIntEx	3.96	10.27	21.30	10.23
TokenEx	-	-	-	-
Token level agreement				
SpanIntEx	66.95	68.71	72.24	67.5
TokenIntEx	66.90	67.29	70.50	65.86
TokenEx	58.07	56.88	61.07	63.10

Table 4: Human Annotation Agreement Results (see §2.3) on the FEVER dataset when explanations are generated based on BERT. The rest of the settings are the same as Table 3.

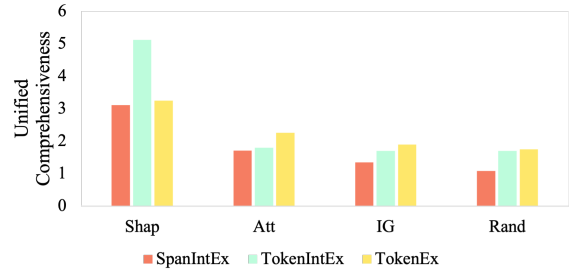
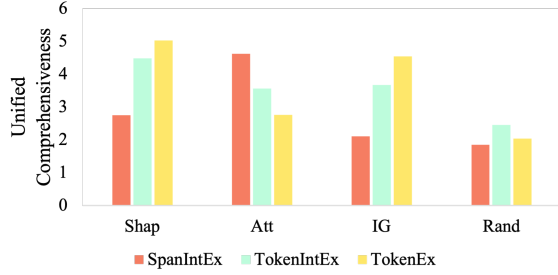
E	Shap	Att	IG	Rand
Interaction level agreement				
SpanIntEx	37.36	47.33	34.18	28.25
TokenIntEx	32.36	35.17	33.06	13.80
TokenEx	-	-	-	-
Token level agreement				
SpanIntEx	80.16	76.28	82.76	70.04
TokenIntEx	84.9	75.92	86.06	75.32
TokenEx	65.74	73.71	70.44	73.34

Table 5: Human Annotation Agreement Results (see §2.3) on SNLI dataset when explanations are generated based on BART. The rest settings are the same as Table 3.

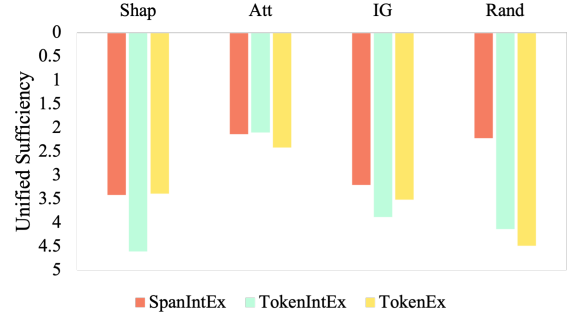
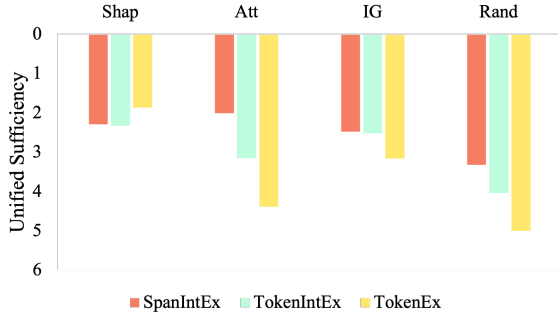
served for TokenIntEx. This suggests that although SpanIntEx and TokenIntEx explanations align more with human reasoning than TokenEx explanations, pairing important tokens or spans into interactions that are plausible to humans remains challenging.

E.3 Simulatability

Regarding insertion formats, for BERT models, text insertion (I_{Text}), which adds explanation text



(a) Comprehensiveness on SNLI dataset, the higher the better. (b) Comprehensiveness on FEVER dataset, the higher the better.



(c) Sufficiency on SNLI dataset, the lower the better.

(d) Sufficiency on FEVER dataset, the lower the better.

Figure 4: Unified Comprehensiveness and Sufficiency of three types of feature attribution explanations on SNLI and FEVER datasets using the BART model. Subfigures (a) and (c) show Unified Comprehensiveness results, while (b) and (d) show Unified Sufficiency results. Explanations are generated by Shapley (Shap), Attention (Att), and Integrated Gradients (IG). Randomly selected span pairs, token pairs, and tokens are baselines corresponding to explanation type `SpanIntEx`, `TokenIntEx` and `TokenEx` and form the group Random baseline (Rand). We set $k = 3$ for top span interactions and adjust token counts as per section §2.2, ensuring the random baseline matches the average token count of the top k span interactions.

E	Shap	Att	IG	Rand
Interaction level agreement				
SpanIntEx	22.86	20.66	18.72	16.76
TokenIntEx	4.71	2.64	10.54	8.64
TokenEx	-	-	-	-
Token level agreement				
SpanIntEx	68.77	65.33	70.22	69.51
TokenIntEx	67.01	63.40	70.98	68.11
TokenEx	59.43	52.15	57.56	60.93

Table 6: Human Annotation Agreement Results (see §2.3) on FEVER dataset when explanations are generated based on BART. The rest settings are the same as Table 3.

to the end of the input sequence, consistently outperforms symbol insertion (I_{Sym}), where symbols are added to the original input sequence, as shown in Tables 7 and 8. However, the opposite effect is observed for BART models, as shown in Tables 9 and 10. This indicates that simulatability results are sensitive to the explanation insertion form, highlighting the need for consistency in insertion form when comparing different explanation types.

E.4 Complexity

D	E	Shap		Att		IG	
		SF	RSF	SF	RSF	SF	RSF
SNLI	SpanIntEx	87.9	3.2	86.7	2.0	88.9	4.2
	TokenIntEx	86.6	1.9	85.3	0.6	85.8	1.1
	TokenEx	87.4	2.7	85.7	1.0	86.0	1.3
FEVER	SpanIntEx	83.9	3.8	85.3	5.2	85.2	5.1
	TokenIntEx	82.7	2.6	84.0	3.9	84.4	4.3
	TokenEx	84.0	3.9	82.3	2.2	81.8	1.7

Table 7: Simulatability results on SNLI and FEVER with BERT as the model used for all explanations $E \in \text{SpanIntEx}, \text{TokenIntEx}, \text{TokenEx}$ generation with attribution method **Shapley**, **Attention**, and **Integrated Gradients** respectively. Note that insertion form I_{Sym} is adopted for combining the explanations and the original input sequence for agent model AM_E , as depicted in §2.4. The agent models used for baseline AM_O , trained without explanations, have simulation F1 scores, as denoted in §2.4, of 84.7% and 80.0% on test set shared with other agent models AM_E , as denoted in §2.4. We set $k = 1$ for top SpanIntEx and calculated the number of top TokenIntEx and TokenEx accordingly as stated in §2.2. The largest increases are highlighted in bold for each dataset with the identical attribution method.

D	E	Shap		Att		IG	
		SF	RSF	SF	RSF	SF	RSF
SNLI	SpanIntEx	87.8	3.1	87.1	2.4	88.2	3.5
	TokenIntEx	86.5	1.8	87.8	3.1	86.4	1.7
	TokenEx	87.0	2.3	86.3	1.6	88.4	3.7
FEVER	SpanIntEx	85.7	5.6	85.1	5.0	86.0	5.9
	TokenIntEx	81.9	1.8	85.6	5.5	84.3	4.2
	TokenEx	85.8	5.7	84.5	4.4	82.0	1.9

Table 8: Simulatability results on SNLI and FEVER with BERT as the model used for all input feature explanation generation. Note that insertion form I_{Text} is adopted for combining the explanations and the original input sequence for agent model AM_E , as depicted in §2.4. The agent models used for baseline AM_O , which are trained without explanations, have simulation F1 scores of 84.7% and 80.0% on the test sets shared with agent model AM_E . The other setting is the same as Table 7

D	E	Shap		Att		IG	
		SF	RSF	SF	RSF	SF	RSF
SNLI	SpanIntEx	87.8	7.9	87.3	7.4	86.5	6.6
	TokenIntEx	83.5	3.6	84.2	4.3	84.6	4.7
	TokenEx	88.2	8.3	81.4	1.5	85.8	5.9
FEVER	SpanIntEx	80.6	7.2	76.1	2.7	75.2	1.8
	TokenIntEx	78.9	5.5	75.9	2.5	74.7	1.3
	TokenEx	80.1	6.7	75.0	1.6	74.1	0.7

Table 9: Simulatability results on SNLI and FEVER with BART as the model used for all input feature explanation generation. Note that insertion form I_{Sym} is adopted for combining the explanations and the original input sequence for agent model AM_E , as depicted in §2.4. The base agent models AM_O trained without explanations have the simulation f1 scores of 79.9% and 73.4%, respectively on the test sets sharing with other agent models AM_E . The other setting is the same as Table 7

D	E	Shap		Att		IG	
		SF	RSF	SF	RSF	SF	RSF
SNLI	SpanIntEx	86.8	6.9	85.0	5.1	84.3	4.4
	TokenIntEx	81.2	1.3	82.6	2.7	81.6	1.7
	TokenEx	83.3	3.4	83.8	3.9	82.2	2.3
FEVER	SpanIntEx	78.2	4.8	75.3	1.9	74.6	1.2
	TokenIntEx	74.8	1.4	74.1	0.7	73.9	0.5
	TokenEx	77.6	4.2	74.9	1.5	73.6	0.3

Table 10: Simulatability results on SNLI and FEVER with BART as the model used for all input feature explanation generation respectively. Note that insertion form I_{Text} is adopted for combining the explanations and the original input sequence for agent model AM_E , as depicted in §2.4. The base agent models AM_O trained without explanations have the simulation f1 scores of 79.9% and 73.4%, respectively. The other setting is the same as Table 7

Dataset	E	Shapley	Attention	IG	R	U
SNLI	SpanIntEx	2.05	1.11	2.10	2.19	2.62
	TokenIntEx	1.72	1.43	2.30	-	-
	TokenEx	2.08	1.64	1.91	-	-
FEVER	SpanIntEx	2.78	2.22	2.90	2.98	3.18
	TokenIntEx	3.12	3.07	3.15	-	-
	TokenEx	2.76	2.22	2.57	-	-

Table 11: Complexity results on SNLI and FEVER datasets for three types of explanations generated by different attribution methods based on BERT model. The **Random** baseline represents the complexity score obtained by randomly generated scores in the range [0,1], ensuring the same number of scores as the number of explanations used. The **Upperbound** is calculated by setting all the attribution scores to the same value while ensuring the same number of scores as the number of explanations used. The lowest complexity score for each specific explanation type compared is highlighted in bold when the explanations are generated by each attribution method.

Dataset	E	Shapley	Attention	IG	R	U
SNLI	SpanIntEx	1.90	1.93	1.63	2.36	2.76
	TokenIntEx	2.50	2.53	2.13	-	-
	TokenEx	1.86	1.95	1.94	-	-
FEVER	SpanIntEx	2.73	3.03	2.38	3.13	3.38
	TokenIntEx	3.30	3.36	2.93	-	-
	TokenEx	2.82	3.07	3.19	-	-

Table 12: Complexity results on SNLI and FEVER datasets for three types of explanations generated by different attribution methods based on BART model. The other settings are the same as Table 11.